CHAPTER 10

THE DISCOVERY OF LOWER ACICULAR FERRITE

10.1 INTRODUCTION

There is general agreement that a weld microstructure primarily containing acicular ferrite will exhibit high strength and excellent toughness due to its small grain size, high dislocation density, and the way in which the plates are dispersed in the microstructure (Pargeter, 1983; Sneider and Kerr, 1984). In contrast, the presence of allotriomorphic ferrite, ferrite plates with aligned carbides, or grain-boundary nucleated bainite is considered detrimental to the toughness of the weld, because these constituents allow cracks to propagate without much deflection. The problem is, in fact, more complicated, since it appears that a microstructure consisting *totally* of acicular ferrite does not exhibit optimum toughness, and that, ideally, a finite amount of allotriomorphic ferrite should also be present in the microstructure (Sneider and Kerr, 1984). Whatever the optimum microstructure, it is clear that a better understanding of the phases involved would permit more detailed investigation on the relationship with mechanical properties. In this context, acicular ferrite is the least understood of all the main phases that occur in steel welds. This work follows on from the work of Yang and Bhadeshia (1987), and Strangwood and Bhadeshia (1987), aimed at identifying and classifying acicular ferrite.

Over many years, the nature of the acicular ferrite phase has been the cause of much speculation. In point of fact, the term "acicular ferrite" is a misnomer. In two dimensions, acicular ferrite appears as randomly-oriented, needle-shaped particles (Figures 10.1a and b), but this belies its true morphology which is that of thin lenticular plates, typically 10μm long and apparently $\sim$ 1μm wide (Bhadeshia, 1987). For a typical low-alloy C-Mn steel weldment, acicular ferrite will begin to appear during cooling in the range 500-440°C (Ito *et al.*, 1982), and its exact nature has, until recently, been a matter for debate. Its ambiguous appearance has sometimes led workers to propose that it is Widmanstätten ferrite (Abson *et al.*, 1978; Cochrane and Kirkwood, 1978). However, a series of experiments (Yang and Bhadeshia 1987; Strangwood and Bhadeshia, 1987), has now shown that acicular ferrite is essentially identical to bainite. It differs morphologically from bainite

a)

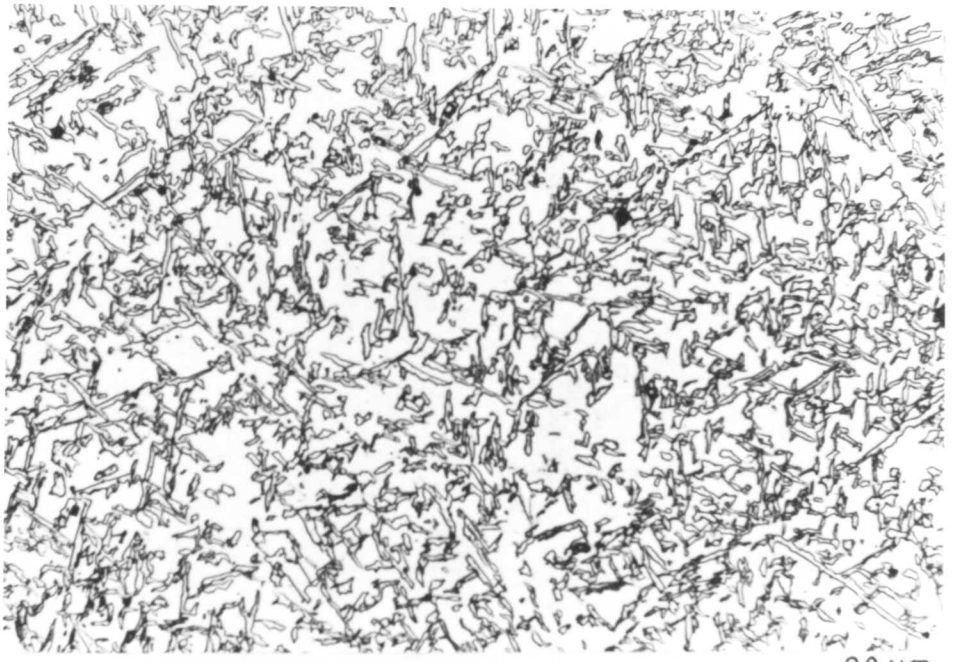

b)

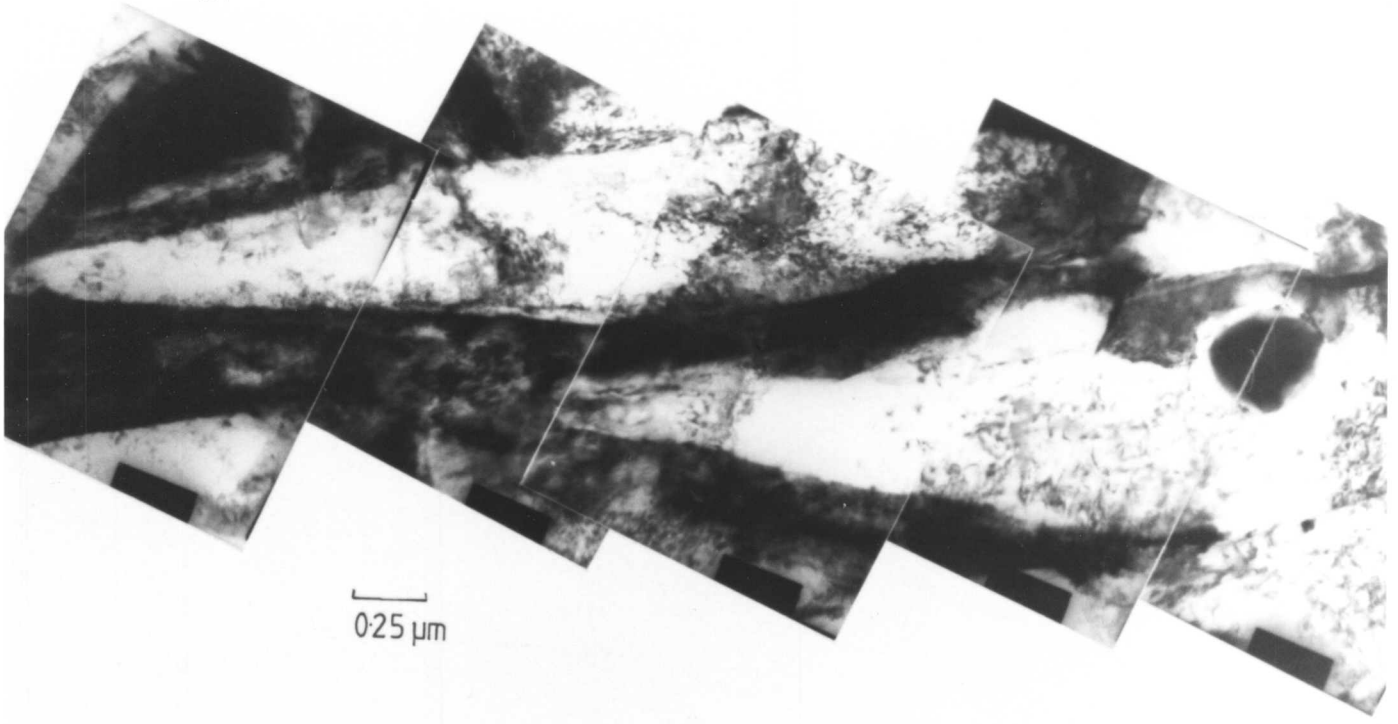

Figures 10.1a and b: Microstructure of acicular ferrite in (a) reaustenitised and isothermally transformed weld metal, and (b) low-C-Mn weld deposit. (After (a) J.-R. Yang (1987), and (b) M. Strangwood (1987), Ph.D. theses, University of Cambridge, U.K.).

found in wrought steels because it nucleates intragranularly on inclusions, and, in low-alloy steel weld deposits, is unable to adopt a sheaf morphology because of physical impingement with other plates nucleated nearby.

In order to put the work that follows in context, it is first instructive to discuss the bainite reaction in steels.

10.2 THE FORMATION OF BAINITE

Bainite forms by the decomposition of austenite at a temperature above the martensite start (M_s), but below that of fine pearlite. Microstructural and kinetic studies can become very complicated since, in low alloy steels, there is considerable overlap between the pearlitic and bainitic temperature ranges. In medium alloy steels, however, the two regions are more distinct, and give isothermal temperature-time-transformation (TTT) diagrams containing two separate C curves. The lower curve usually exhibits a flat top, and this corresponds to the bainite start (B_s) temperature (Zener, 1946).

Bainite grows in the form of sheaves of lenticular platelets of ferrite separated by regions of austenite (γ), martensite (α'), or cementite (θ). The ferrite plates have a thickness of about $0.5 - 0.7\mu$m (Oblak and Hehemann, 1967), although this varies with transformation temperature and alloy composition. The transformation is accompanied by a shape change which is an invariant-plane strain (I. P. S.) (Speich, 1962), and the bainitic subunits have the same, or nearly the same, crystallographic orientation with respect to one another.

Bainite is found in two district morphologies: upper bainite and lower bainite. Upper bainite consists of platelets of ferrite which are adjacent to one another, and in very nearly the same orientation in space. The ferrite platelets have the same habit plane (Ohmori, 1971; Sandvik, 1982) and comprise a sheaf which has a thin wedge plate morphology in three dimensions (Bhadeshia and Edmonds, 1980), as shown in Figure 10.2. The sheaves nucleate at austenite grain boundaries and have a rational orientation relationship (*i.e.* Kurdjumov-Sachs and Nishiyama-Wasserman type) with the austenite. Since upper bainite forms at higher temperatures when the yield strength of austenite is relatively low, plastic relaxation of the shape change leads to a high dislocation density in the surrounding ferrite (Bhadeshia and Edmonds, 1979).

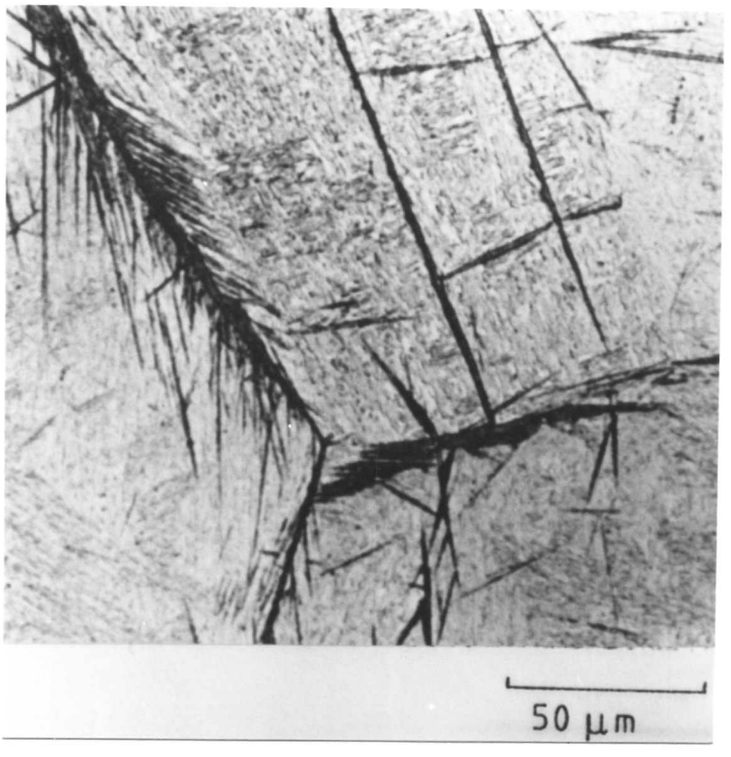

Figure 10.2: Upper bainite in high silicon steel, formed after isothermal transformation within the bainitic region. (After H. K. D. H. Bhadeshia (1979), Ph.D. thesis, University of Cambridge, U.K.).

Lower bainite is distinguished from upper bainite by the presence of carbide precipitation within the constituent ferrite subunits. These carbides, when they are cementite, precipitate in a variant of the Pitsch orientation within a subunit (Shackleton and Kelly, 1967), frequently at about 60° to the subunit long direction, the single variant arising from the need to minimise strain energy (Bhadeshia, 1980). Thorough crystallographic analysis (Bhadeshia, 1980) has shown the absence of the expected three phase $\alpha - \gamma - \theta$ orientation relationship, indicating that the carbides do not form by interphase precipitation. They might, therefore, precipitate either from the austenite during transformation, or from supersaturated ferrite. The low solubility of carbon in ferrite relative to austenite suggests intuitively the latter mechanism, and becomes an unavoidable conclusion of the discussion below.

A noteworthy feature of the bainite transformation is the phenomenon of incomplete reaction (Bhadeshia and Edmonds, 1980; Christian and Edmonds, 1984) in which, provided no interfering secondary reactions occur, transformation within the bainite range is found to produce only a limited amount of bainitic ferrite, the maximum extent of transformation increasing from zero with undercooling below the B_s temperature. Cessation of the reaction occurs before the carbon content of the remaining austenite reaches the equilibrium value calculated by extrapolating the Ae_3 curve. This incomplete reaction phenomenon can be understood thermodynamically (Bhadeshia and Edmonds, 1980). The reaction stops when it is thermodynamically impossible to obtain composition invariant transformation. This condition is described by the T_o curve on the phase diagram, which defines the locus of all temperatures where austenite and ferrite of the same composition have the same free energy. For the bainite reaction, the matrix will tend to physically restrain the shape change due to transformation from austenite, and this gives rise to a strain and surface energy of approximately 400 J/mol. Consequently a new T_o curve, T_o', may be defined to include the effects of this stored energy of 400 J/mol. This curve is at slightly lower carbon concentrations than the T_o curve, and any displacive diffusionless transformation must occur below it. In a similarly way, a no-substitutional partitioning (Ae_3') curve, for which transformation occurs without the redistribution of substitutional alloying elements, can be defined. Figure 10.2 shows dilatometric results obtained in low alloy C-Si steels in which cementite formation is inhibited allowing the true final content of the carbon in the austenite to be measured. Both the upper and lower bainite reaction were observed to terminate when the residual austenite composition reached the T_o' curve. The ex-

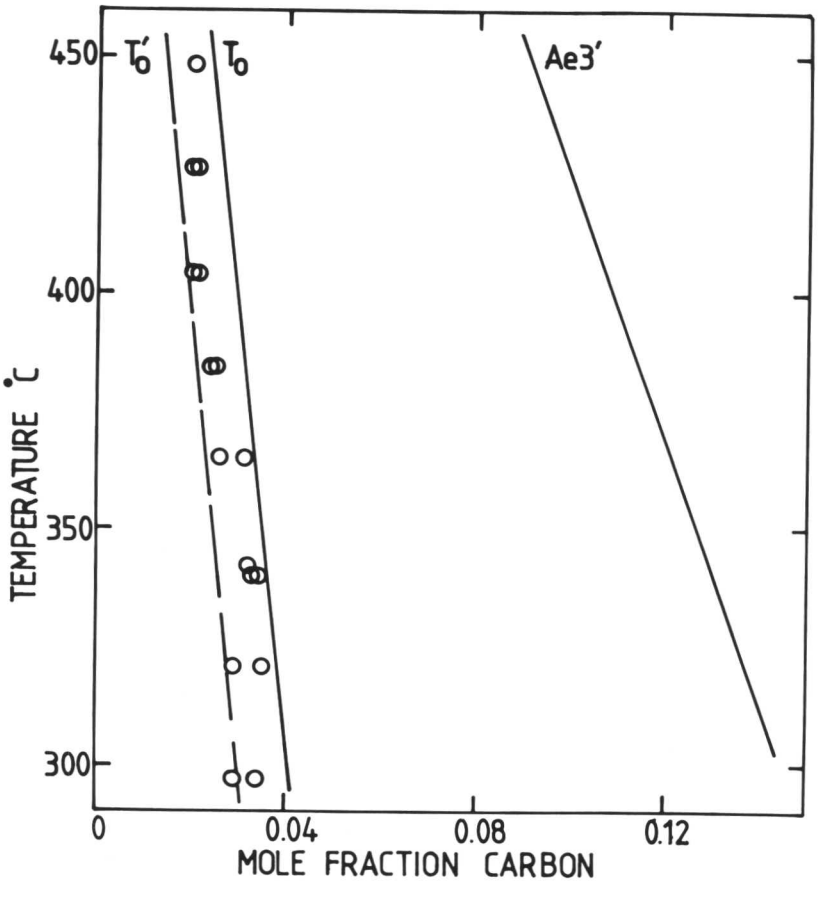

Figure 10.3: Thermodynamic analysis of the bainite transformation. The Ae_3' line indicates the position of the no-substitutional partitioning (paraequilibrium) curve. Dilatometric analysis (o) shows the austenite carbon content at the termination of the bainite reaction to be in good agreement with the T_o' curve. (After H. K. D. H. Bhadeshia and D. V. Edmonds (1980), *Acta Metall.*, **28**, 1265-1273).

planation for the incomplete reaction phenomenon, therefore, is that the bainitic ferrite forms with a supersaturation of carbon, which subsequently diffuses into the surrounding austenite. This means that the next subunit to form will do so from austenite which is enriched with carbon, and so under a reduced driving force. Bainite formation stops when sufficient carbon has diffused into the austenite that the b.c.c. and f.c.c. structures of the same composition have the same free energy. The fact that for some of the points in Figure 10.3 the amount of transformation exceeds that theoretically predicted can, in part, be attributed to later evidence (Bhadeshia and Waugh, 1982) that an inhomogeneous distribution of carbon exists during transformation, leading to a greater amount of reaction than that calculated on the basis of the average carbon content of the residual austenite. Reynolds *et al.* (1984) interpret these results qualitatively in terms of a solute drag effect at the α/γ interface. However, their mechanism is not clearly explained, and much other research relating to the formation of bainite is also incompatible with a diffusional, and strongly supportive of a displacive transformation mechanism. This includes the following observations:

- Prolonged holding at the bainite reaction temperature has been observed to yield pearlite *after* the bainite reaction (Bhadeshia and Edmonds, 1979).

- The growth rate of bainite, monitored *in situ* using photo-emission electron microscopy (Bhadeshia, 1984) has been observed to be many orders of magnitude higher than that expected from carbon-controlled growth.

- Field ion microscopy (Bhadeshia and Waugh, 1982) has shown there to be a uniform distribution of substitutional alloying elements at the transformation interface. The complete absence of substitutional solute segregation mean that solute drag models are not tenable.

In summary, therefore, the bainite transformation seems to be described best by a displacive transformation mechanism. The bainite subunits form in an initial f.c.c.$\rightarrow$b.c.c. transformation involving an I. P. S. shape change. This gives rise to surface relief and a characteristic habit plane and orientation relationship. At this stage the bainitic ferrite has a composition identical to that of the surrounding austenite. Subsequently, the regions of residual austenite between the platelets of ferrite decompose either diffusionally to cementite (or other carbides) and ferrite, or partially decompose to martensite during cooling to ambient temperature with

carbon partitioning into the residual austenite. For lower bainite, which forms at lower temperatures than upper bainite, the process of partitioning of carbon into the residual austenite is expected to be slower, and hence some of the excess carbon precipitates within the bainitic ferrite. ϵ-carbide or θ precipitates form to relieve the carbon supersaturation within the bainitic ferrite. After nucleation at an austenite grain boundary, new platelets form autocatalytically on the pre-existing platelets to give the aggregation of platelets that comprise the classical bainite sheaves (Bhadeshia, 1987).

10.3 ACICULAR FERRITE

Acicular ferrite exhibits an incomplete reaction phenomenon during transformation, with the amount of reaction tending to zero as the temperature is raised towards the B_s temperature (Yang and Bhadeshia, 1987). The lenticular plates of acicular ferrite (α_a) form by the same displacive mechanism as bainite, with the carbon redistributing into the austenite subsequent to the transformation. However, they adopt a different morphology because nucleation occurs intragranularly at inclusions within the grains, and also because sheaf growth is restricted by hard impingement with plates nucleated at adjacent sites.

The purpose of the present work was to confirm further the mechanism of acicular ferrite growth. There are no carbide particles found within acicular ferrite in steel weld deposits, so that it is better described as *upper* bainite. However, if the carbon concentration of the weld is increased (with an associated decrease in transformation temperature), then it should, by analogy with the bainite transformation in wrought steels, be possible to observe "lower acicular ferrite", which is identical to upper acicular ferrite except that it is expected to contain a particular kind of cementite precipitation with the ferrite.

10.4 EXPERIMENTAL METHOD

In order to be able to expect to see intragranularly-nucleated lower bainite, an unusual weld would have to be fabricated. Yang and Bhadeshia (1987) found that an acicular ferrite morphology was favoured when the grain size was large, and the inclusion content was high - both conditions likely to promote intragranular nucleation by providing a relatively high density of suitable heterogeneous nucle-

ation sites, and forestall impingement from grain boundary phases also forming as a consequence of austenite decomposition. Conversely, bainitic microstructures are found in welds when the alloy content is high, the oxygen content is low, and the austenite grain size is large. The first of these is expected to be the most powerful factor in influencing microstructure. However, unfortunately, highly-alloyed welds often give microstructures that are very difficult to interpret (Deb *et al.*, 1987). Therefore a weld with a high (0.3 wt%) carbon content was chosen as the simplest way by which lower bainite could be expected to be seen. The concentration of the other alloying elements was kept deliberately low in order to facilitate microstructural interpretation.

Although a low weld metal oxygen context could lead to the generation of bainitic microstructures, by depriving the interior of the columnar grains of nucleation sites for acicular ferrite, this was not desired, since the experiment aimed to isolate intragranularly-nucleated, rather than grain-boundary nucleated, bainite. However, the oxygen content should not be high either, since multiple nucleation events would lead to hard impingement between plates, masking the morphology of the product phase. In light of this, an oxygen content in the range 100-200ppm seemed desirable.

An ISO-2560 multirun manual-metal-arc weld was fabricated from 200mm thick plate. The arc current and voltage were 180A and 23V respectively with DC positive electrode polarity and no preheat. The welding speed was approximately 4mm/s. In accordance with the specification, the maximum interpass temperature was 250°C. The carbon content of the weld metal was controlled using specially-designed 4mm diameter carbon-coated electrodes to give a weld metal whose composition is given in Table 10.1.

C	Si	Mn	Cr	Ni	Mo	P	S	O	N
0.32	0.48	1.65	0.03	0.03	0.01	0.011	0.005	0.0141	0.0064

Table 10.1: Weld 10.1: Weld metal composition analysis (wt%)

It can be seen that the oxygen content is within the range intended.

Electrolytic etching of the weld metal was carried out in an aqueous solution of 20% NaOH by volume, at a voltage of 10 volts, for 45 seconds. Thin foils for transmission electron microscopy were prepared from 3mm diameter discs machined

from the top (unreheated) bead of the weld. The discs were ground sequentially on 400, 1200 and 4000 mesh SiC paper to a thickness of 0.05mm, and then electrochemically profiled using a twin-jet Fischione electropolisher. Polishing was carried out at a voltage of 40V and at room temperature, in an electrolyte of 5% perchloric acid/ 25% glycerol in ethanol.

10.5 RESULTS

Figure 10.4 shows the solidification microstructure of the top bead of the weld. As was discussed in Chapter 2, because of the high cooling rates found in MMA welding, a carbon content of 0.30 wt% or greater will be liable to induce solidification from the melt as austenite in a low-alloy steel, rather than δ-ferrite. That solidification occurred as austenite is confirmed by the strong directionality of the microstructure due to unrestricted grain growth in the liquid phase, and by the fact that the cells within the grains change orientation only at the columnar boundaries. Near the weld centreline, which was the region of the weld that solidified last, a transition from a cellular to cellular-dendritic morphology can be observed, resulting from a build-up of solute ahead of the solidifying interface.

Figure 10.5 shows details of the microstructure with the specimen etched in nital. The cell boundaries can be seen to delineated by a discontinuous phase. The interior of the cells is difficult to resolve. Hardness testing was used to help characterize the microstructure. The hardness of the specimen (Vickers 10kg) was found to be (with a 95% confidence) 299 ± 2.2HV. Using a Zeiss microhardness tester, the dark region of the weld metal structure (*i.e.* the microstructure within the cells) gave a hardness of 448 ± 32HV. However, microhardness measurements of the discontinuous grain boundary phase gave a reading of 664 ± 36HV. This indicates that although the cell boundary phase superficially resembles allotriomorphic ferrite, it is martensitic in nature. In fact, martensitic formation at cell boundaries can be seen in high strength weld deposits, due to the large amount of solute segregation that occurs during solidification (Grong and Matlock, 1986). However, this does not appear to have been seen previously in low C-Mn welds. The most likely reason is that low-alloy steels usually solidify as δ-ferrite when the resultant alloying element segregation is not great. In this work, however, solidification occurred as primary austenite, which characteristically results in a much larger amount of chemical microsegregation, making martensitic formation at the cell boundaries

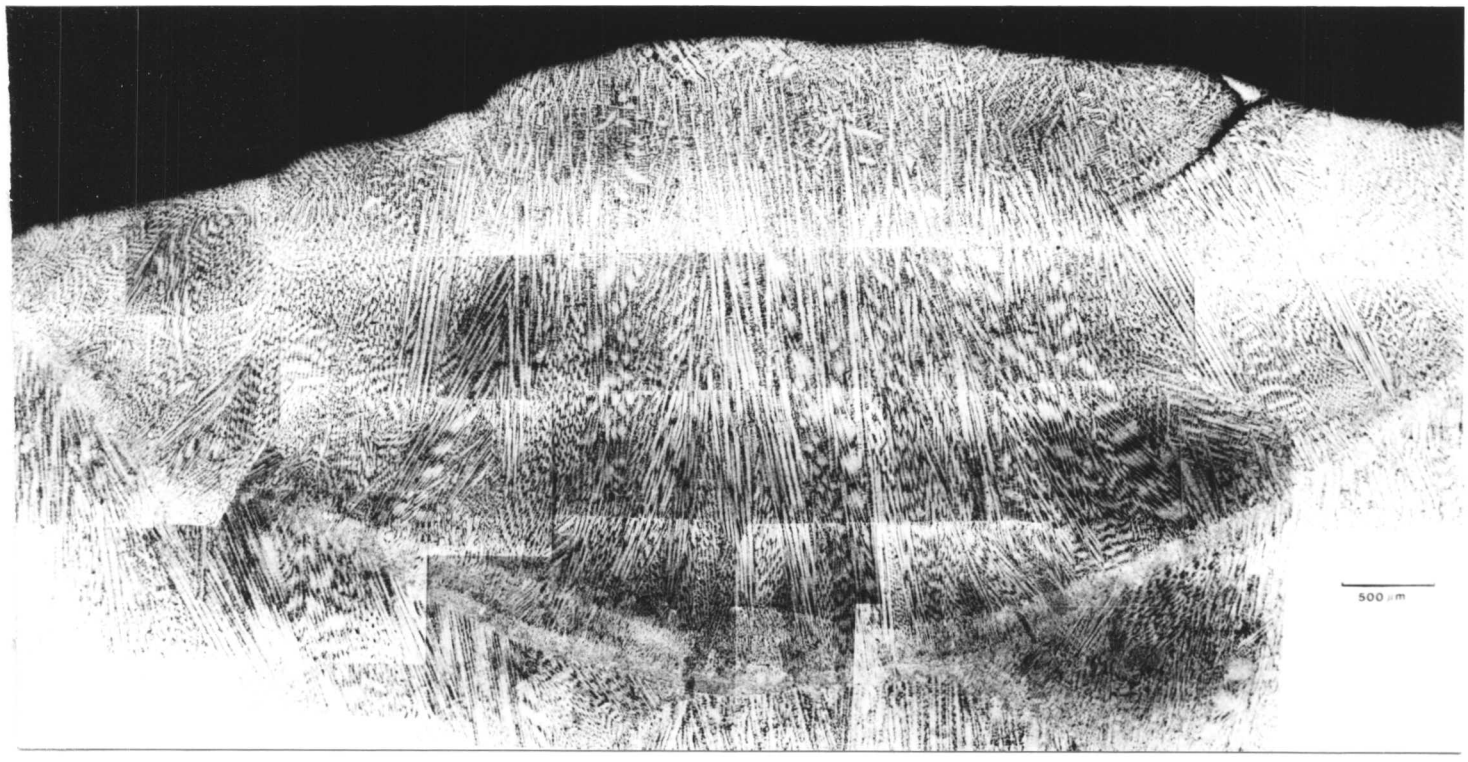

Figure 10.4: Weld metal microstructure showing solidification structure. Lightly electrolytically etched in saturated aqueous sodium hydroxide, followed by 2% nital.

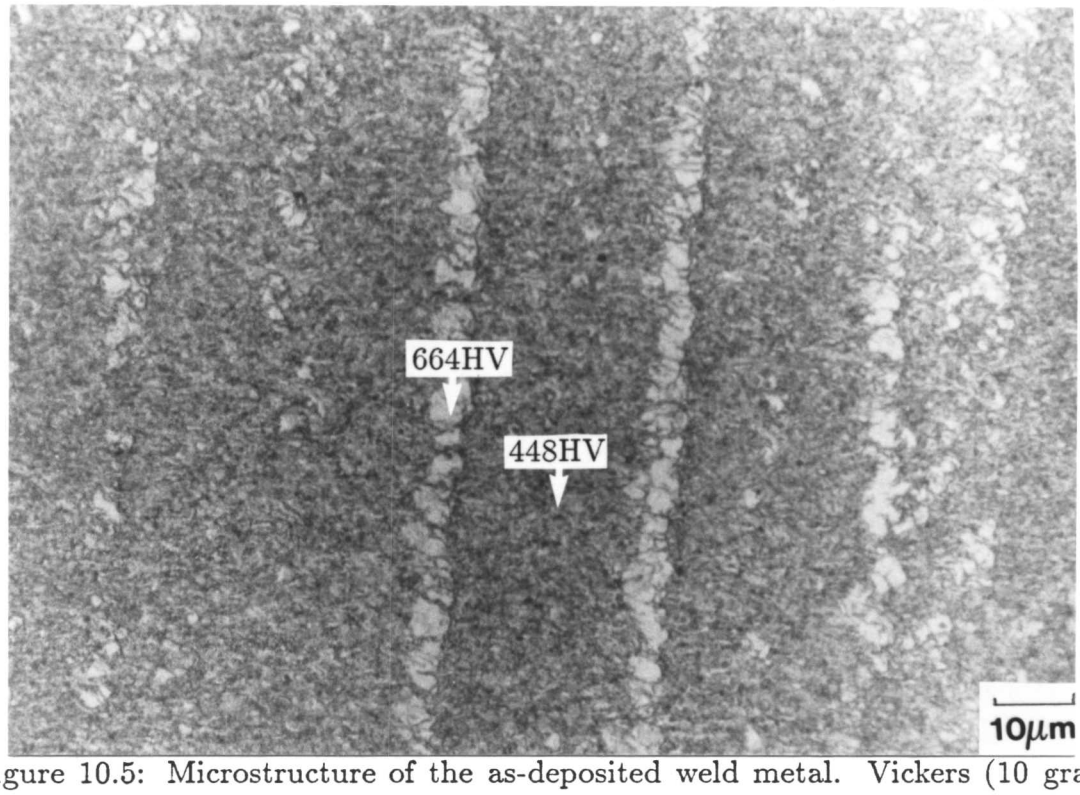

Figure 10.5: Microstructure of the as-deposited weld metal. Vickers (10 gram) hardnesses are indicated for cell boundaries, and for the weld metal microstructure between them. Etchant: 2% nital.

more likely.†

The weld proved difficult to etch, probably because of its unusual composition, and, as will be seen later, profuse cementite precipitation. However, the microstructure of the weld was successfully revealed by electrolytic etching in saturated aqueous sodium hydroxide (Figures 10.6a and b), and a dilute preparation of nital, when the weld was found to contain a large amount of fine-grained acicular ferrite. Inclusions can also be seen in Figure 10.6a located at the cell boundaries, thus confirming earlier work described in Chapter 3.

Transmission electron micrographs of the weld are given in Figures 10.7-10.14. The microstructure of the weld metal at the prior austenite grain boundaries consisted predominantly of grain boundary nucleated upper bainite, as shown in Figures 10.7a and b. The high alloy concentration and high amount of solute segregation associated with solidification as austenite meant that allotriomorphic ferrite formation was inhibited, and this led to a microstructure at the grain boundaries completely different to that normally encountered in low-carbon C-Mn weld deposits where allotriomorphic ferrite and Widmanstätten ferrite are the predominant phases.

Within the columnar grains, the usual platelets of acicular ferrite, which are

---

†It will be noted that the microhardness readings of the individual phases are both higher than that of the weld as a whole. This occurs are a consequence of the so-called "indentation size effect". It is an observed phenomenon that hardness measurements obtained from a material increase with decreasing load (O'Neill, 1967; Sargent, 1986). Although this behaviour has been explained for single crystals (Upit and Varchenya, 1973), it is not fully understood why polycrystalline materials should behave in this manner. One reason may be that friction is playing a part. Alternatively, for large deformations, grains partly slip over one another, so that the resultant deformation area is increased slightly. Generally, this effect goes unnoticed. However, the microhardness measurements in this work had to be made using the smallest available load to ensure that the indent size was much less than the dimensions of the cell boundary phase. The applied load was, therefore, only 1/1000th the macroload of 10kg, and this caused the observed hardness to increase. However, the comparison made between the hardnesses of the two phases recorded for the same applied load is still quite valid.

a)

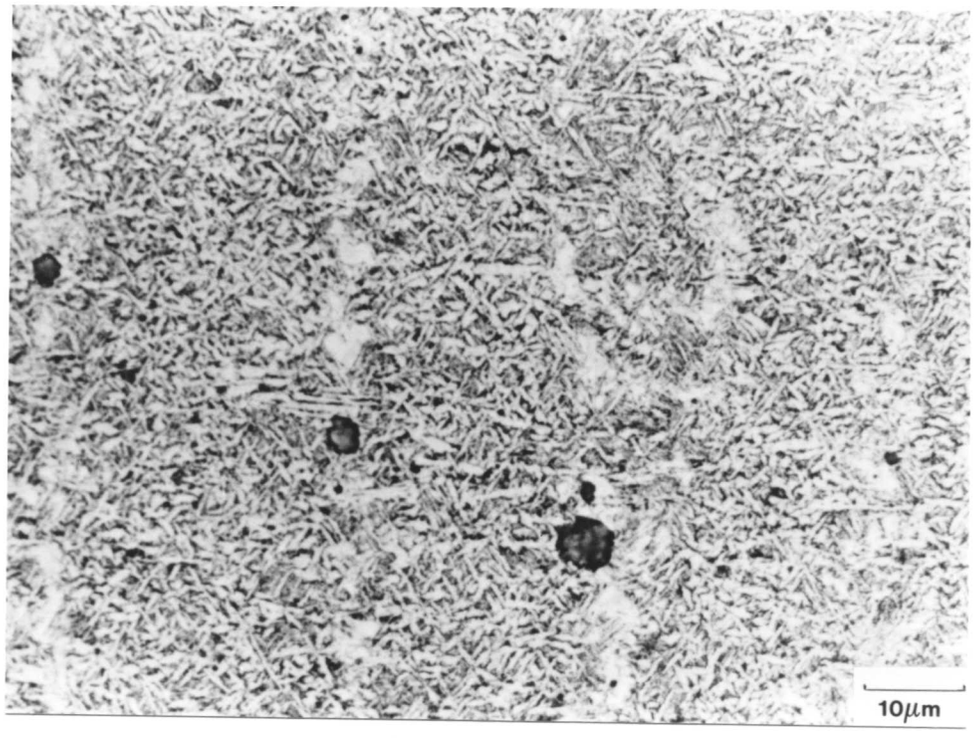

b)

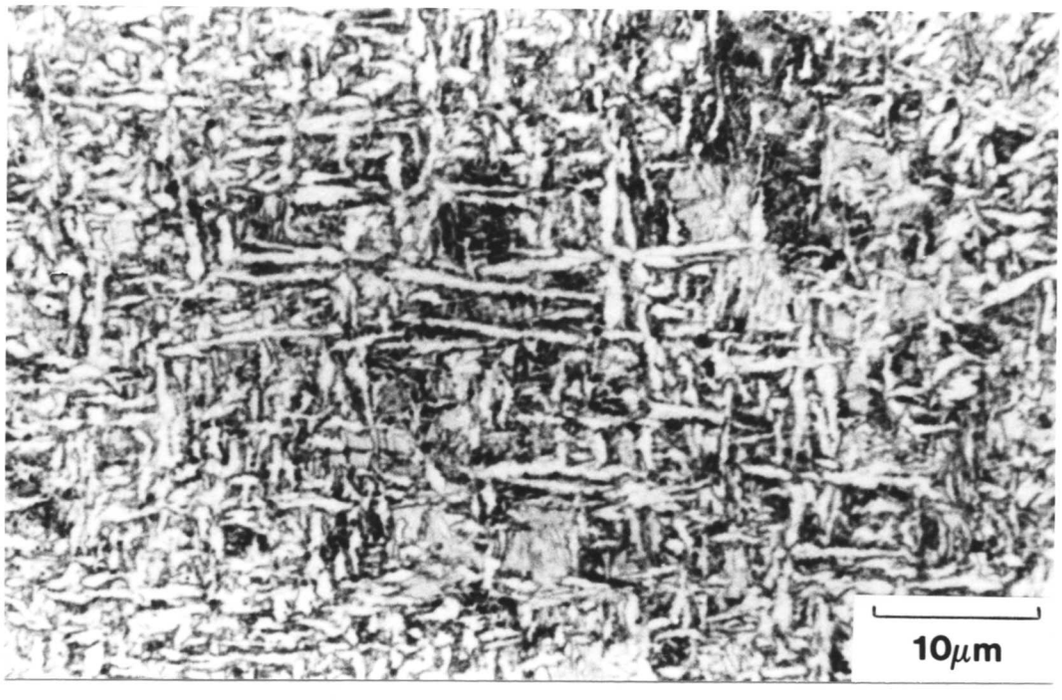

Figures 10.6a and b: Weld 10.1: Details of the as-welded microstructure. (a) electrolytically etched in saturated aqueous sodium hydroxide, and (b) etched in 0.5% nital.

a)

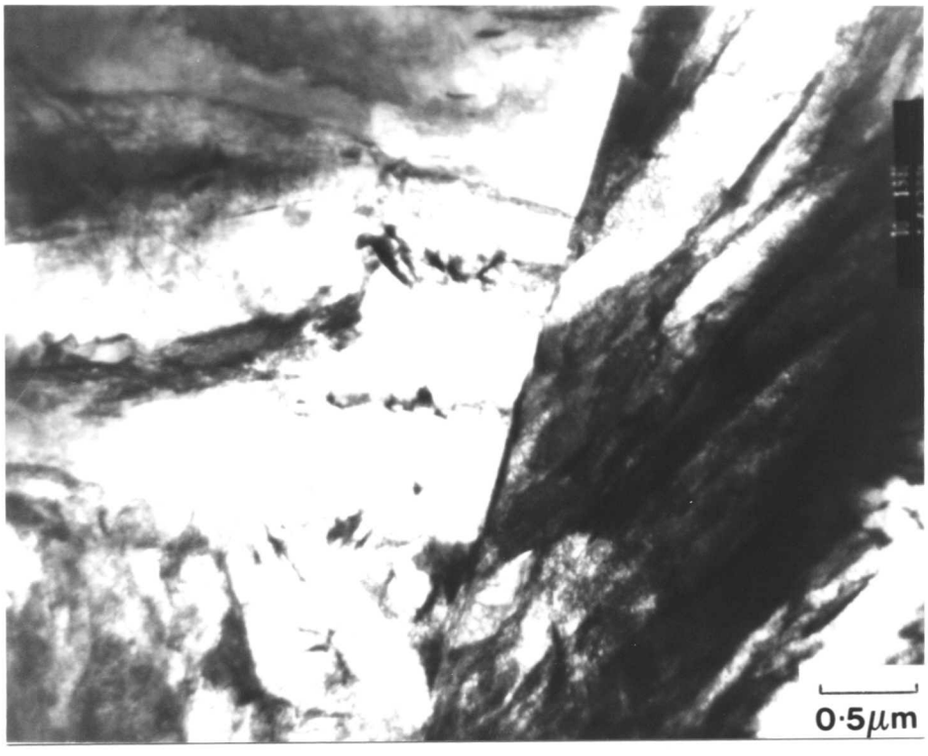

b)

Figures 10.7a and b: Classical bainite subunits nucleated at the prior austenite grain boundaries of Weld 10.1. The grey phase between the subunits in Figure 7a is likely to be retained austenite. Lower bainitic carbides (arrowed) may be seen within the ferrite, towards the top right of Figure 7b.

an instantly recognizable feature of low-carbon weld deposits were present, corresponding to intragranularly-nucleated bainite (Figure 10.8a). Other bainitic subunits appear to have nucleated around these laths in the same way that the formation of acicular ferrite in low-carbon C-Mn weld deposits is characterised by the sympathetic nucleation of α_a on pre-existing laths. Further evidence of the bainitic nature of the microstructure is given in Figure 10.8b.

In addition to the conventional acicular ferite platelets, spectacular formations of intragranularly-nucleated "lower acicular ferrite" plates were also observed (Fig. 10.9). These were in all respects identical to conventional acicular ferrite, except that each plate contained a single orientation variant of cementite precipitates inclined to the plate axis. The cementite particles exhibited a Bagaryatski orientation relationship with the ferrite in which they precipitated. The microstructure of the lower acicular ferrite plates was found to be exactly identical to that of lower bainite in wrought steels, except that the clusters of plates nucleated at inclusions are not in the form of sheaves. The fact that a mixed microstructure of carbide-free acicular ferrite (*i.e.* intragranularly-nucleated upper bainite), and lower acicular ferrite (*i.e.* intragranularly-nucleated lower bainite) was observed, is probably a reflection of the fact that the microstructure formed by continuous cooling transformation.

Figures 10.10 and 10.11a and b show another region from the weld metal, emphasizing the large amount of cementite precipitation that has taken place within the bainitic ferrite. Figure 10.12a shows a high magnification micrograph of the the lower bainitic microstructure, comprising carbides within heavily dislocated ferrite. Figure 10.12b demonstrates that the carbides exhibit a Bagarystski orientation relationship with the ferrite. Of all the phases that may form during the cooling of austenite, this orientation relationship is specific to lower bainite, and so proves the identity of the phase. Further details of the as-welded microstructure are shown in Figures 10.13 and 10.14.

10.6 DISCUSSION

The growth of lower bainite in a weld in the manner of intragranularly-nucleated plates has been hitherto unseen. The development of this highly unusual microstructure may be interpreted as being a consequence of the relatively high amount of carbon present in the weld, for, in general, a high carbon concentration will lead to an increased likelihood of bainite formation. Figure 10.15 shows a

a)

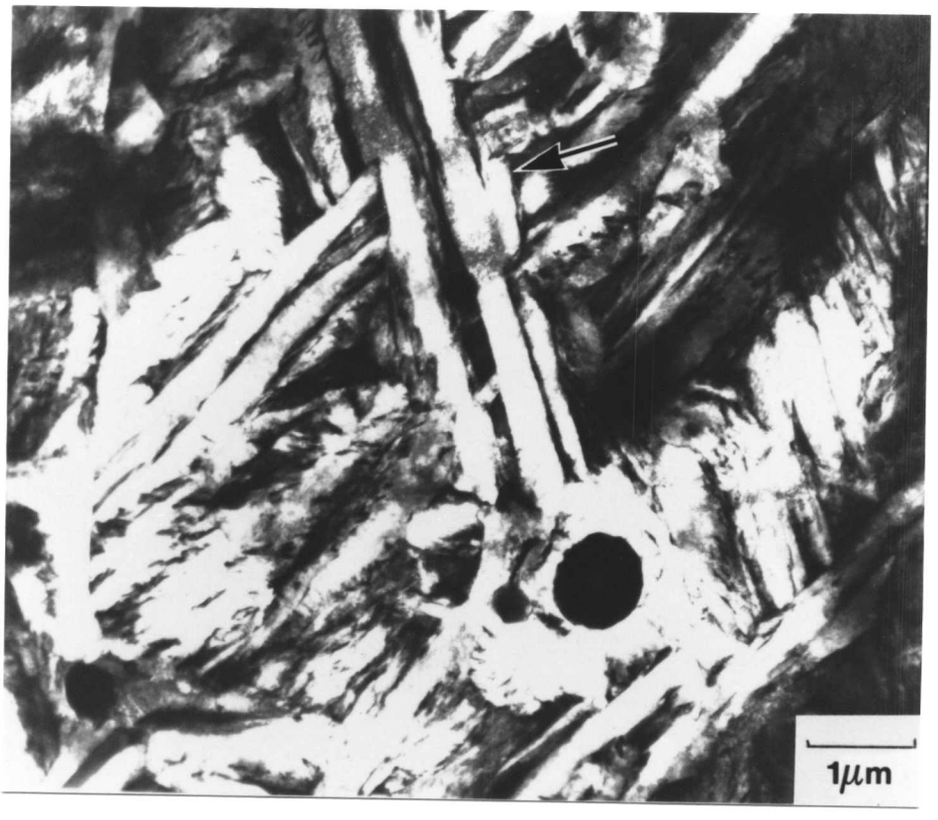

b)

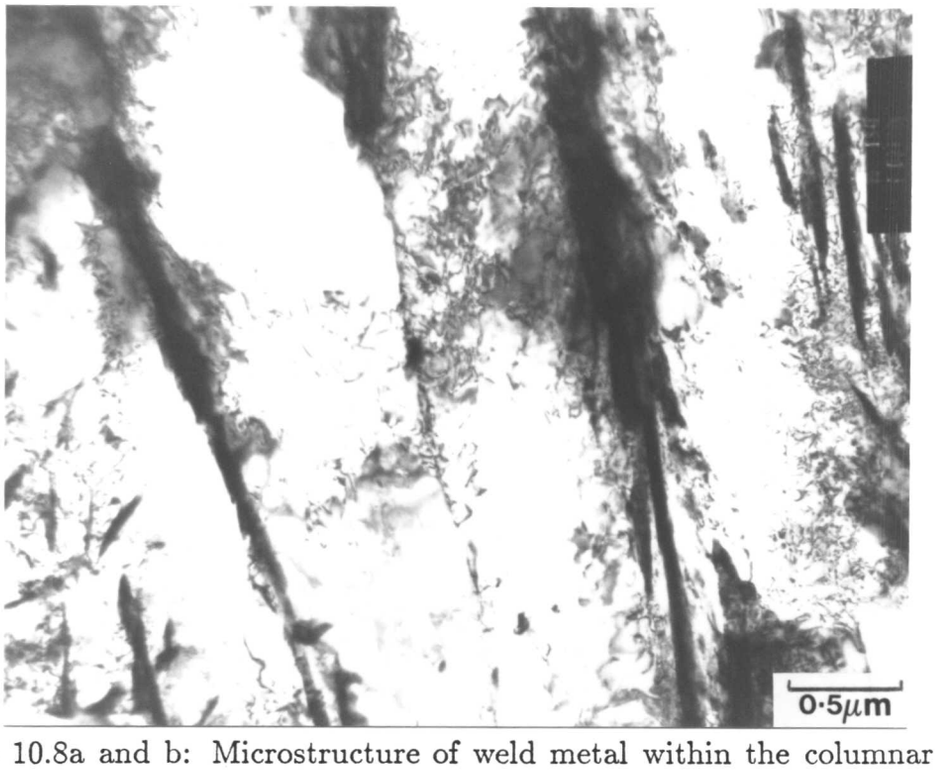

Figures 10.8a and b: Microstructure of weld metal within the columnar grains, showing (a) long parallel subunits, comprising bainitic sheaf (arrowed), apparently nucleated on inclusion, and (b) higher magnification micrograph of bainitic sheaves.

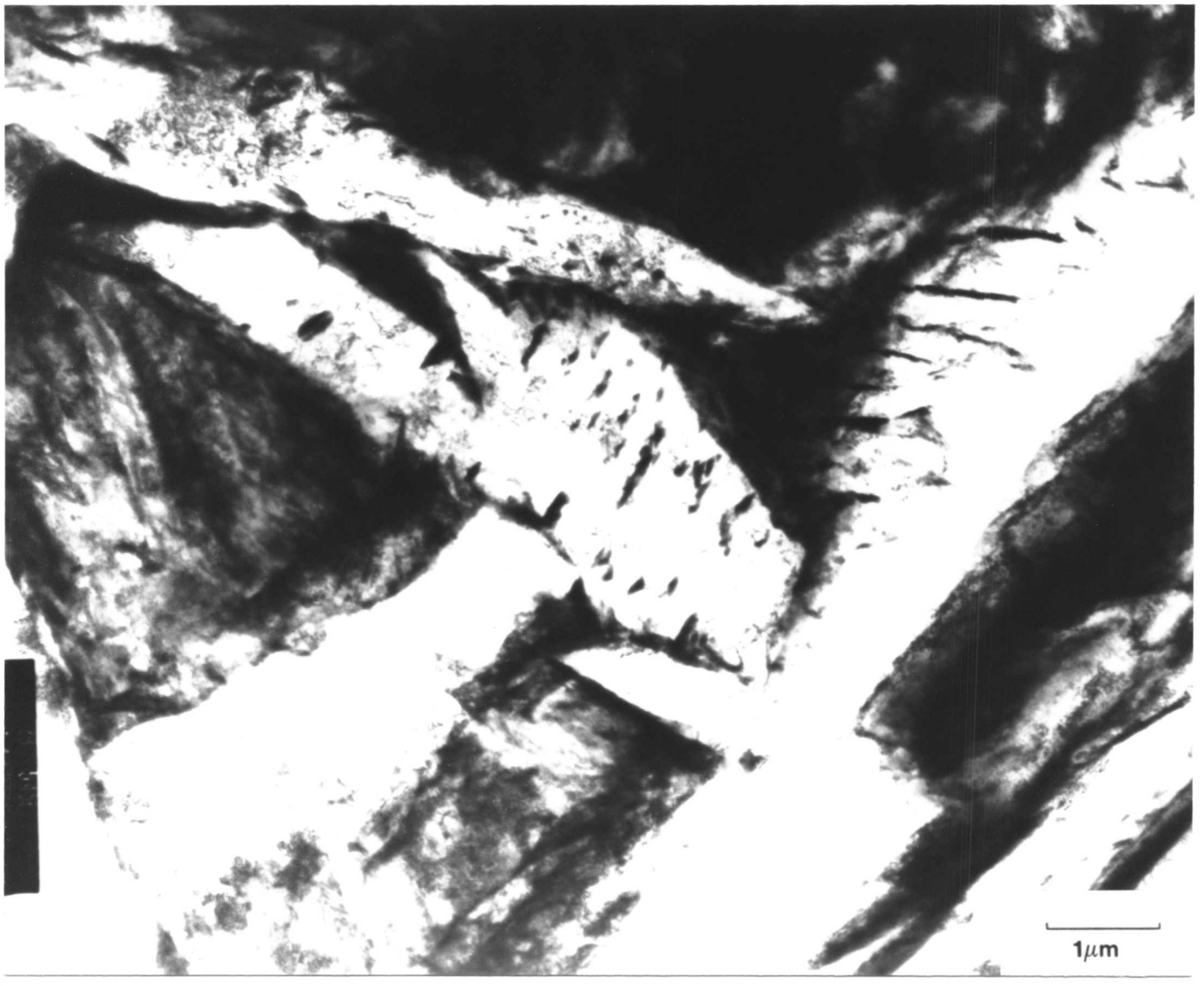

Figure 10.9: Weld metal microstructure showing lower acicular ferrite.

Figure 10.10: Photo-montage of the microstructure of Weld 10.1 within the columnar grains showing classical lower bainitic microstructure.

a)

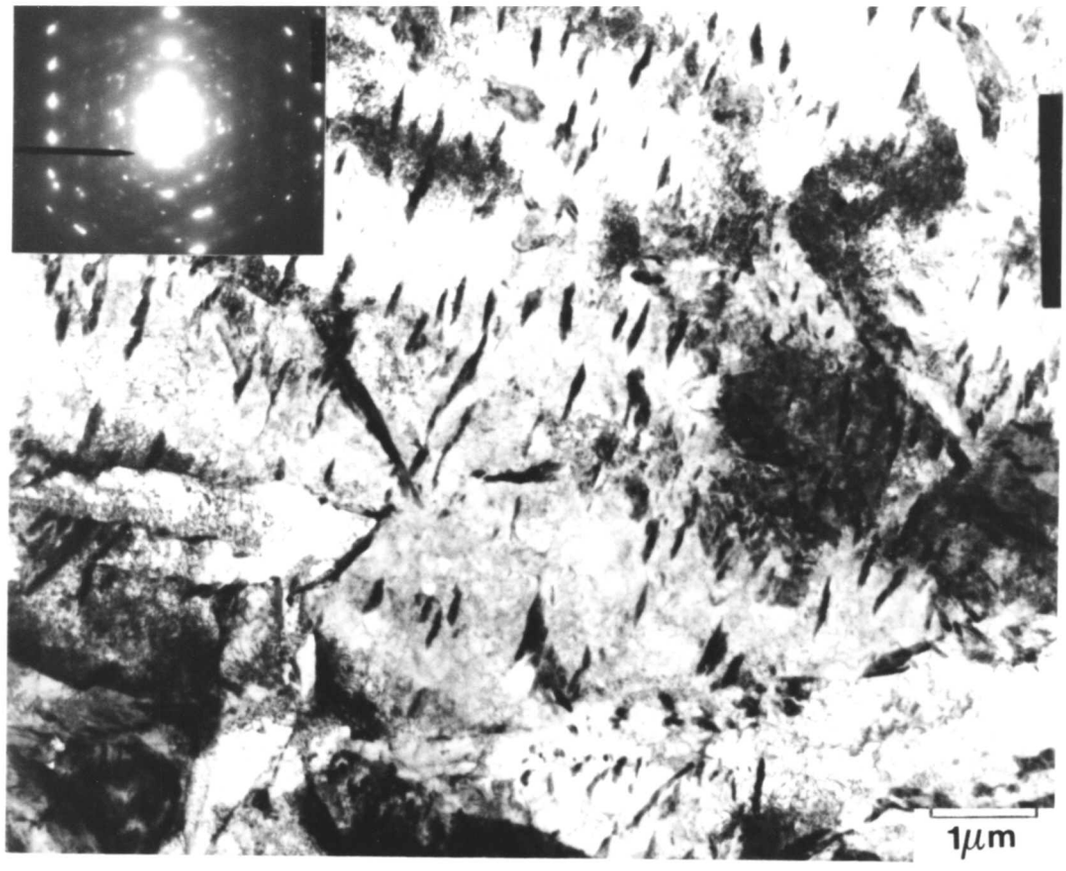

b)

Figures 10.11a and b: (a) Bright field image of weld metal microstructure, and (b) diffraction pattern taken from $(0\bar{1}3)$ cementite spot.

a)

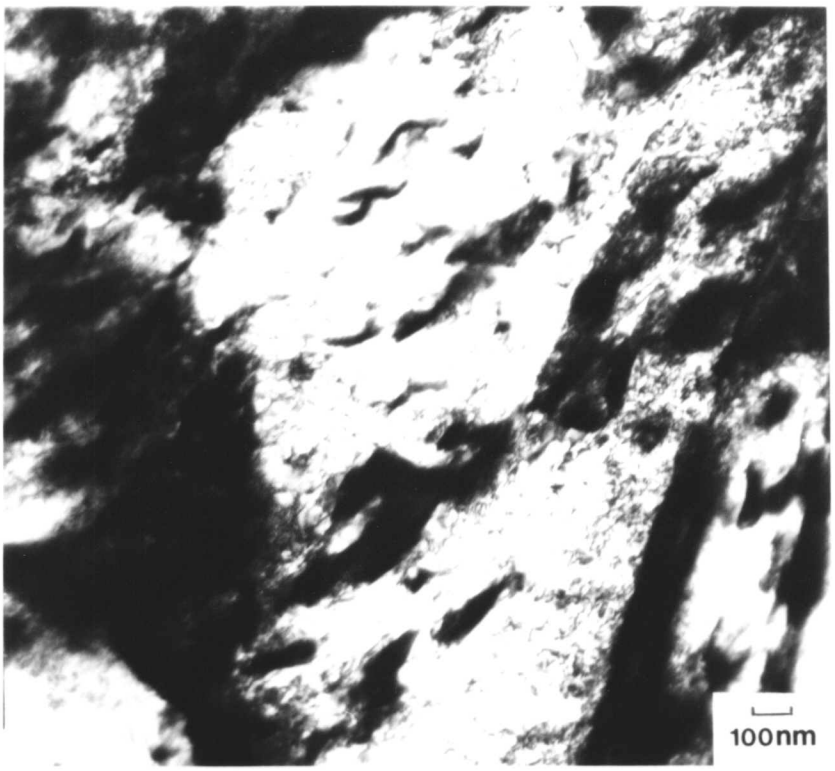

b)

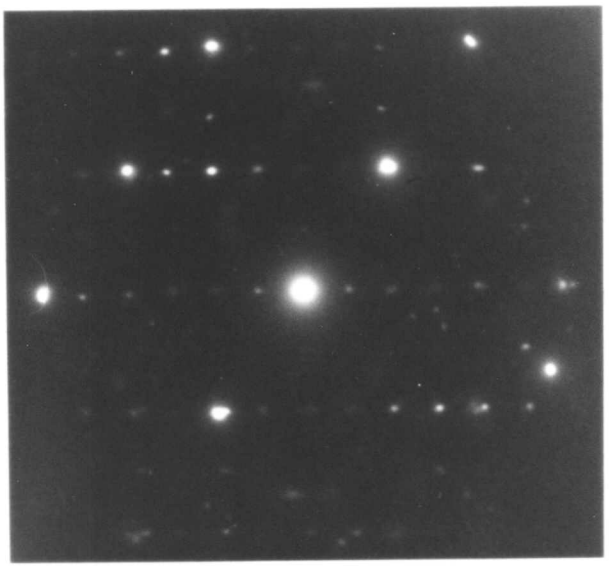

c)

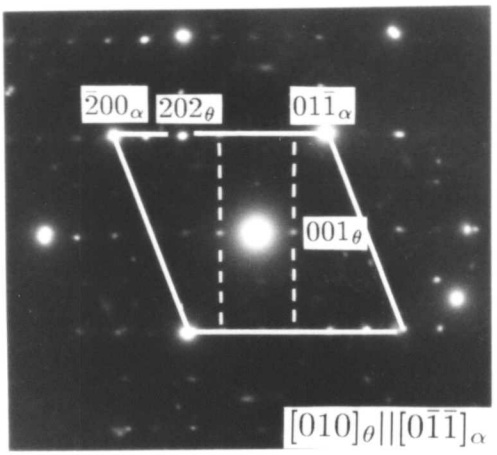

Figures 10.12a-c: (a) High magnification micrograph showing carbides within ferrite matrix, (b) diffraction pattern, and (c) interpretation of diffraction pattern. The carbides exhibit a Bagaryatski orientation relationship with the ferrite matrix.

a)

b)

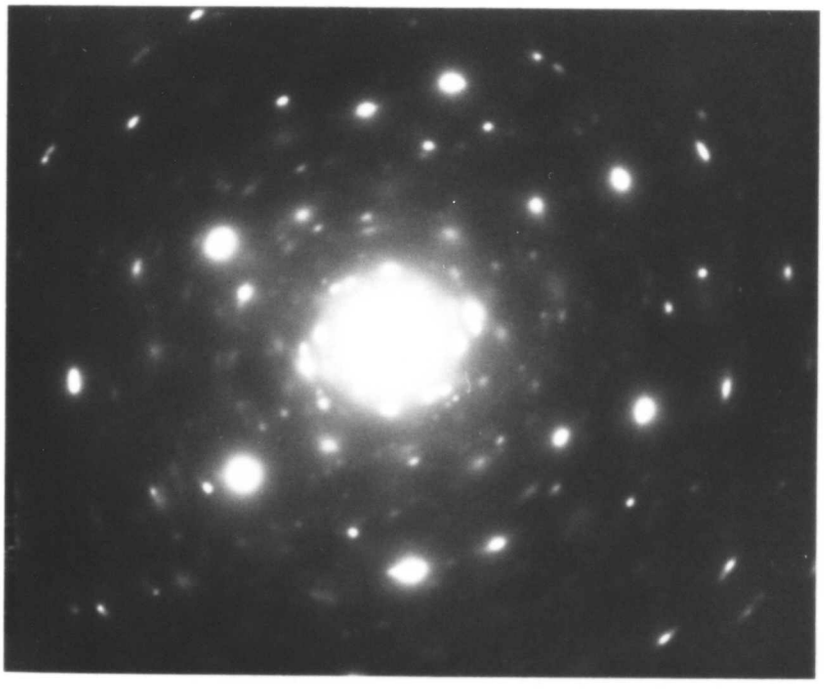

c)

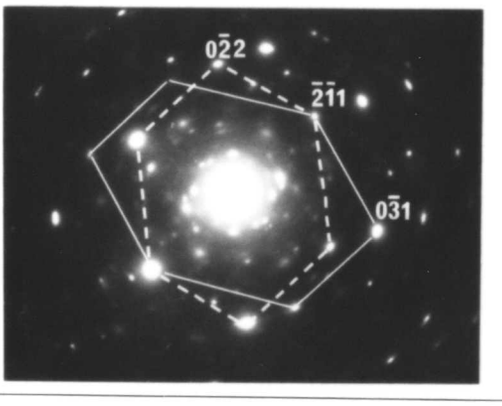

Figures 10.13a-c: (a) Micrograph of bainitic subunits with carbides within them, (b) diffraction pattern, and (c) interpretation of diffraction pattern, showing two adjacent ferrite plates have an $[0\bar{1}\bar{1}]||[\bar{1}1\bar{3}]$ orientation relationship.

Figure 10.14: Micrograph quintessentialising the microstructure of Weld 10.1. The micrograph shows a spherical oxide inclusion surrounded by bainitic ferrite. Sub-units of upper and lower bainite may both be seen. Note the high dislocation density within the upper bainite.

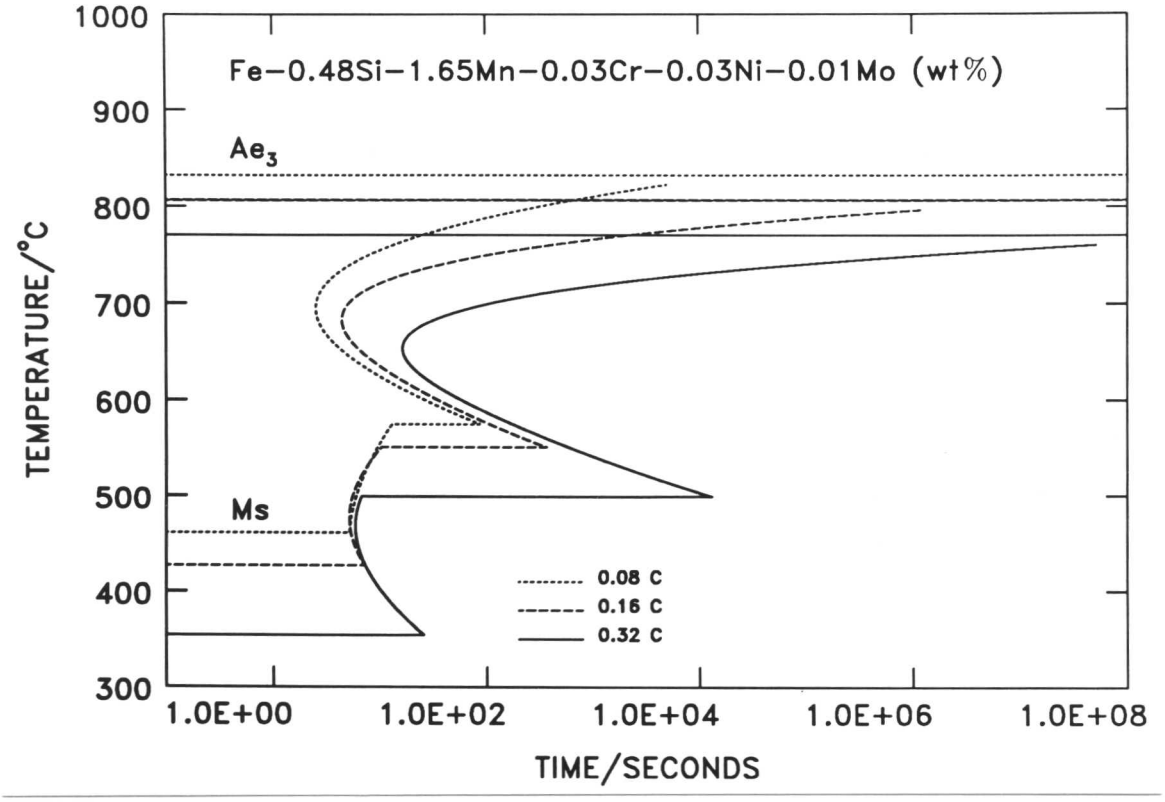

Figure 10.15: Isothermal time-temperature-transformation diagrams for a steel with the same composition as Weld 10.1, and for compositionally equivalent steels with 0.08 and 0.16 wt%C. Calculated after the method due to Bhadeshia (1982).

calculated isothermal time-temperature-transformation (TTT) diagram for a steel with the same composition as Weld 10.1, and compares this with TTT curves calculated for steels with one half and one quarter the carbon concentration of the weld metal. [The curves are calculated using a program due to Bhadeshia (1982), which is based on a modification of Russell's nucleation work (1968; 1969)]. Although Figure 10.13 should only be interpreted qualitatively, since, in reality, weld deposits are chemically inhomogeneous, and austenite decomposition occurs by continuous cooling, nevertheless, the retardation of the pearlite start temperature, and increased prominence of the bainitic region for increasing carbon concentrations can clearly be seen, showing that bainite formation in Weld 10.1 is possible, and not unexpected.

Since it is necessary to distinguish between the two bainitic phases observed, it is, therefore, proposed that they should be referred to as upper acicular ferrite, and lower acicular ferrite. Upper acicular ferrite is identical to the acicular ferrite habitually found in low-carbon weld deposits. Lower acicular ferrite has not been seen before, and corresponds to ferrite that has nucleated on inclusions, or sympathetically on laths of either upper or lower acicular ferrite, during continuous cooling of the weld. It is the phase that would be seen if the weld were to be reaustenitised, and isothermally transformed in the lower bainitic region.

10.7 SUMMARY

The microstructure of an ISO-2560 geometry 0.32C-1.65Mn-0.48Si (wt%) manual-metal-arc weld has been examined optically, and in the transmission electron microscope. The as-welded structure was found to consist of straight prior austenite grains which has solidified as the primary phase. Microhardness measurements demonstrated that the cell boundaries of the weld metal microstructure were largely martensitic, the martensite forming as a consequence of the relatively large amount of chemical segregation that results from austenitic solidification.

Transmission electron microscopy revealed that the microstructure of the weld was predominantly bainitic. Upper bainite was found nucleated at the grain boundaries, and as sheaves within the columnar grains. In the latter case, nucleation appeared to have occurred initially on inclusions. A large part of the microstructure consisted of lower bainite, which is a phase that is completely uncharacteristic of low-carbon weld deposits. The lower bainite formed due to the increasing difficulty

of carbon diffusion, and the carbon enrichment of the austenite, that occurred as the weld cooled. The likelihood that lower bainite will nucleate intragranularly on inclusions to form acicular ferrite in the same manner as upper bainite has led to the submission of a new nomenclature. It is suggested that upper bainitic acicular ferrite, which is the acicular ferrite phase habitually found in low-alloy steel weld deposits, be referred to as upper acicular ferrite when necessary to contrast it with acicular ferrite which formed as lower bainite. The latter should more precisely be referred to as lower acicular ferrite.

REFERENCES

ABSON, D. J., DOLBY, R. E., and HART, P. H. M. (1978), "Trends in Steels and Consumables for Welding", *[Proc. Conf.]*, Welding Institute, Abington, U.K., 75-101.

BHADESHIA, H. K. D. H. (1979), Ph.D. thesis, University of Cambridge. U.K.

BHADESHIA, H. K. D. H. (1980), *Acta Metall.*, **28**, 1103-1114.

BHADESHIA, H. K. D. H. (1982), *Met. Sci.*, **16**, (3), 159-165.

BHADESHIA, H. K. D. H. (1984), "Phase Transformations in Ferrous Alloys", *[Proc. Conf.]*, Eds., A. R. Marder and J. I. Goldstein, The Metallurgical Society of A. I. M. E., Warrendale, Pa., 15086, 335-339.

BHADESHIA, H. K. D. H. (1987), Review on bainite in steels, in "Phase Transformations 1987", *[Proc. Conf.]*, Institute of Metals, London, U.K., in press.

BHADESHIA, H. K. D. H. and EDMONDS, D. V. (1979), *Metall. Trans. A*, **10A**, (7), 895-907.

BHADESHIA, H. K. D. H. and EDMONDS, D. V. (1980), *Acta Metall.*, **28**, 1265-1273.

BHADESHIA, H. K. D. H. and WAUGH, A. R. (1982), *Ibid.*, **30**, 775-784.

CHRISTIAN, J. W. and EDMONDS, D. V. (1984), "Phase Transformations in Ferrous Alloys", *[Proc. Conf.]*, Eds., A. R. Marder and J. I. Goldstein, The Metallurgical Society of A. I. M. E.,Warrendale, Pa., 15086, 293-325.

COCHRANE, R. C., and KIRKWOOD, P. R. (1978), "Trends in Steels and Consumables for Welding", *[Proc. Conf.]*, Welding Institute, Abington, U.K., 103-121.

DEB, P., CHALLENGER, K. D., and THERRIEN, A.E. (1987), *Metall. Trans. A.*, **18A**, 987-999.

GRONG, O. and MATLOCK, D. R. (1986), *Int. Met. Rev.*, **31**, 27-48.

ITO, Y., NAKANISHI, M., and KOMIZO, Y. (1982), *Met. Constr.*, (9), 472-378.

OHMORI, Y. (1971), *Trans. I. S. I. J.*, **11**, 95-101.

O'NEILL, H. (1967), "Hardness Measurements of Metals and Alloys", Chapman and Hall Ltd., London, 43-44.

PARGETER, R. J. (1983), *Weld. Inst. Res. Bull.*, (7), 215-220.

REYNOLDS, W. T., ENOMOTO, M., and AARONSON, H. I. (1984) "Phase

Transformations in Ferrous Alloys", *[Proc. Conf.]*, Eds., A.R. Marder and J.I. Goldstein, The Metallurgical Society of A. I. M. E., Warrendale, Pa., 15086, 155-200.

RUSSELL, K. C. (1968), *Acta Metall.*, **16**, 761-769.

RUSSELL, K. C. (1969), *Ibid.*, **17**, 1123-1131.

SANDVIK, B. P. J. (1982), *Metall. Trans. A*, **13A**, 777-787.

SARGENT, P. M. (1986), "Microindentation Techniques in Materials Science and Engineering", *[Proc. Conf.]*, Eds., P. J. Blau and B. R. Lawns, A. S. T. M., Philadelphia, 160-174.

SHACKLETON, D. N. and KELLY, P. M. (1967), *Acta Metall.*, **15**, 979-992.

SNEIDER, G. and KERR, H. W. (1984), *Canad. Metall. Q.*, **23**, (3), 315-325.

SPEICH, G. R. (1962), "Decomposition of Austenite by Diffusional Processes", *[Proc. Conf.]*, Eds., V. F. Zackay and H. I. Aaronson, Interscience, New York, 353-370.

STRANGWOOD, M. (1987), Ph.D. thesis, University of Cambridge, U.K.

STRANGWOOD, M. and BHADESHIA, H.K.D.H. (1987), "Advances in Welding Science and Technology", ASM International, Ohio, *[Proc. Conf.]*, 209-213.

SVENSSON, L.-E. and BHADESHIA, H.K.D.H. (1988), International Conference of the International Institute of Welding, to be presented.

UPIT, G. P. and VARCHENYA, S. A. (1973), "The Science of Hardness Testing, and its Research Applications", *[Proc. Conf.]*, Eds., J. H. Westbrook and H. Conrad, A. S. M., Metals Park, Ohio, 135-144.

YANG, J.-R. (1987), Ph.D. thesis, University of Cambridge, U.K.

YANG, J.-R. and BHADESHIA, H.K.D.H. (1987), "Advances in Welding Science and Technology", A. S. M. International, Ohio, *[Proc. Conf.]*, 187-191.

ZENER, C., (1946), *Trans. A. I. M. M. E.*, **167**, 550-595.